Japan, for permitting the use of the cytofluorograph.

References

Balhorn, R., Chalkley, R., & Granner, D. (1972) *Biochemistry 11*, 1094–1098.
Bradbury, E. M., Inglis, R. J., & Matthews, H. R. (1974a) *Nature (London) 247*, 257–261.
Bradbury, E. M., Inglis, R. J., Matthews, H. R., & Langan, T. A. (1974b) *Nature (London) 249*, 553–556.
Davidson, R. L., & Gerald, P. S. (1976) *Somatic Cell Genet. 2*, 165–176.
Gurley, L. R., Walters, R. A., & Tobey, R. A. (1973) *Biochem. Biophys. Res. Commun. 50*, 744–750.
Gurley, L. R., Walters, R. A., & Tobey, R. A. (1974a) *J. Cell Biol. 60*, 356–364.
Gurley, L. R., Walters, R. A., & Tobey, R. A. (1974b) *Arch. Biochem. Biophys. 164*, 469–477.
Gurley, L. R., Walters, R. A., & Tobey, R. A. (1975) *J. Biol. Chem. 250*, 3936–3944.
Gurley, L. R., D'Anna, J. A., Barham, S. S., Deaven, L. L., & Tobey, R. A. (1978) *Eur. J. Biochem. 84*, 1–15.
Hildebrand, C. E., & Tobey, R. A. (1975) *Biochem. Biophys. Res. Commun. 63*, 134–139.
Hohmann, P., Tobey, R. A., & Gurley, L. R. (1976) *J. Biol. Chem. 251*, 3685–3692.
Lake, R. S., & Salzman, N. P. (1972) *Biochemistry 11*, 4817–4826.
Lake, R. S., Goidl, J. A., & Salzman, N. P. (1973) *Exp. Cell Res. 73*, 113–121.
Marks, D. B., Paik, W. K., & Borun, T. W. (1973) *J. Biol. Chem. 248* 5660–5667.
Marunouchi, T., & Nakano, M. M. (1980) *Cell Struct. Funct. 5*, 53–66.
Marunouchi, T., Yasuda, H., Matsumoto, Y., & Yamada, M. (1980) *Biochem. Biophys. Res. Commun. 95*, 126–131.
Matsumoto, Y., Yasuda, H., Mita, S., Marunouchi, T., & Yamada, M. (1980) *Nature (London) 284*, 181–183.
Mita, S., Yasuda, H., Marunouchi, T., Ishiko, S., & Yamada, M. (1980) *Exp. Cell Res. 126*, 407–416.
Ord, M. G., & Stocken, L. A. (1969) *Biochem. J. 112*, 81–89.
Panyim, S., & Chalkley, R. (1969) *Arch. Biochem. Biophys. 130*, 337–346.
Shepherd, G. R., Noland, B. J., & Hardin, J. M. (1971) *Arch. Biochem. Biophys. 142*, 299–302.
Slevely, W. S., & Stocken, L. A. (1968) *Biochem. J. 110*, 187–191.

Double-Resonance Experiments at 500 MHz on Gene-5 Protein and Its Complex with Octadeoxyriboadenylic Acid†

N. C. M. Alma,* B. J. M. Harmsen, W. E. Hull,‡ G. van der Marel,§ J. H. van Boom,§ and C. W. Hilbers*

ABSTRACT: In this paper, a detailed description is presented of the aromatic part of the 500-MHz ^1H nuclear magnetic resonance (NMR) spectrum of the helix-destabilizing gene-5 protein (GVP) encoded by the coliphage M13. As a result of the resolution obtained at 500 MHz, it was possible to perform selective decoupling and time-resolved selective Overhauser experiments. The magnitudes of the observed Overhauser effects compare favorably with magnitudes expected on the basis of theoretical calculations. These experiments in conjunction with selective decoupling experiments allowed a detailed interpretation of the aromatic part of the protein spectrum. The spectrum of the aromatic part of the GVP–$d(A)_8$ complex could be interpreted in a similar fashion. The ring protons of one phenylalanyl residue and of two tyrosyl residues show rather large shifts upon complex formation. This indicates that these residues are involved in the interaction with the DNA molecule in accordance with earlier observations. Direct evidence for the proximity of these aromatic rings and the DNA fragment in the complex was obtained by additional Overhauser experiments. It turns out that the H_3', H_4', and/or the H_5' sugar protons of the oligonucleotide are situated near the ring protons of (most likely) two or all three of the aromatic residues of which the resonances undergo large shifts upon complex formation.

Gene-5 protein (GVP)[1] is a DNA helix-destabilizing protein, encoded by the filamentous *Escherichia coli* phages M13 fl and fd. It is synthesized in great amounts in the infected *E. coli* cell and plays an essential role in the replication process of the phage, in which it induces a changeover from replicative form (RF) replication to single-stranded viral DNA synthesis (Alberts et al., 1972; Oey & Knippers, 1972; Ray, 1977).

Information about the structure of the protein and the protein–DNA complex has been obtained from various physicochemical experiments. The protein has a molecular weight of 9690 and exists in solution predominantly as a dimer (Pretorius et al., 1975; Cavalieri et al., 1976). The amino acid sequence has been determined (Cuyper et al., 1974; Nakashima et al., 1974a,b). Recently, the X-ray structure of the protein has been determined to 2.3-Å resolution (McPherson et al., 1979, 1980b). A 30-Å long groove in the protein structure is presumed to be the DNA binding region. The elucidation of the X-ray structure of a protein–oligonucleotide complex is in progress (McPherson et al., 1980a). Both the in vivo and the in vitro complexes of GVP with the viral DNA

† From the Department of Biophysical Chemistry, University of Nijmegen, Nijmegen, The Netherlands. *Received December 9, 1980.* This research was supported by the Netherlands Foundation for Chemical Research (SON) with financial aid from the Netherlands Organization for the Advancement of Pure Research (ZWO). The NMR experiments were performed in the laboratory of Bruker Analytische Messtechnik, Rheinstetten-Forchheim, Federal Republic of Germany.

‡ Bruker-Physik AG, Rheinstetten-Forchheim, Federal Republic of Germany.
§ Department of Organic Chemistry, University of Leiden, Leiden, The Netherlands.

[1] Abbreviations used: DSS, 4,4-dimethyl-4-silapentane-1-sulfonate; FID, free induction decay; GVP, gene-5 protein; NMR, nuclear magnetic resonance; NOE, nuclear Overhauser effect; RF, replicative form.

0006-2960/81/0420-4419$01.25/0

have been visualized in the electron microscope (Alberts et al., 1972; Pratt et al., 1974). Both complexes are rod shaped and consist of two antiparallel nucleoprotein chains, but they differ in axial repeat distance and in width. The protein binds to DNA in a stoichiometry of about four nucleotides per protein monomer (Alberts et al., 1972; Pretorius et al., 1975; Cavalieri et al., 1976; Day, 1973), the binding being strongly cooperative. Nitration experiments have shown that tyrosyl residues 26, 41, and 56 are situated at the protein surface but become inaccessible for nitration when the protein binds to DNA (Anderson et al., 1975). Fluorescence, circular dichroism, and NMR studies also indicate that surface tyrosines are involved in DNA binding (Pretorius et al., 1975; Day, 1973; Garssen et al., 1977, 1978; Coleman et al., 1976; Coleman & Armitage, 1977). In addition, recent NMR studies have shown that at least one phenylalanyl residue plays a role in the binding process (Hilbers et al., 1978; Garssen et al., 1980; Coleman & Armitage, 1978). These aromatic amino acids are presumed to stack upon the DNA bases.

These conclusions were based on experiments carried out at 270 and 360 MHz. The experiments were performed under solution conditions where the protein is mainly present as a dimer. Although the molecular weight of this species is still relatively low, the measured spectra exhibited insufficient resolution so that only a few individual resonances could be assigned (Garssen et al., 1978, 1980; Hilbers et al., 1978; Coleman & Armitage, 1978). Raising the temperature to improve the spectra is not feasible because at higher temperatures, i.e., above 40 °C, the protein rapidly denatures.

In this paper, we describe the elucidation of the aromatic part of the ^{1}H NMR spectrum of the protein using 500-MHz NMR. The improved resolution obtained at this frequency permits a detailed study of this spectrum using selective decoupling and NOE experiments. In the same way, the aromatic ^{1}H NMR spectrum of the protein–d$(A)_8$ complex is examined, yielding detailed insight into the changes occurring upon protein–DNA complex formation. For the protein–d$(A)_8$ complex, NOE experiments show that saturation of adenyl ring protons and sugar H_1' protons causes a change of magnetization at certain aromatic ring protons of the protein. This demonstrates that these latter protons are close to the oligonucleotide in the protein–d$(A)_8$ complex. These results confirm the conclusions regarding the involvement of the phenylalanyl and tyrosyl residues in the protein–DNA interaction drawn in this and earlier papers.

Materials and Methods

Materials. The isolation and purification of GVP were essentially as described previously (Garssen et al., 1977). The protein concentration was determined from the absorption at 276 nm with a molar absorption coefficient of 7100 M^{-1} cm^{-1} (Day, 1973). For NMR measurements, the protein solution was concentrated by ultrafiltration and lyophilized 2 times from 99.75% D_2O.

The octanucleotide d$(A)_8$ was synthesized with the phosphotriester method (Arentzen et al., 1979; G. van der Marel and J. H. van Boom, unpublished experiments). It was used as the Na^+ salt. Excess salt was removed by passage over a Sephadex G-10 column. For concentration determination, a molar absorption coefficient at 260 nm of 8.25×10^4 was used. This number was obtained via a phosphorus determination (Böttcher et al., 1971). For NMR measurements, the oligonucleotide was lyophilized 3 times from 99.75% D_2O. All other materials were of reagent grade.

Instrumentation. Ultraviolet absorption measurements were carried out with a Zeiss PMQ II spectrophotometer. The pHs reported are the uncorrected pH meter readings in D_2O solutions.

^{1}H NMR spectra at 500 MHz were recorded on a Bruker WM-500 spectrometer operating in the Fourier-Transform mode with four-phase quadrature detection. Chemical shifts are quoted relative to DSS. Downfield shifts are defined as positive. Spectra were resolution enhanced by a Lorentzian to Gaussian transformation (Ernst, 1966; Ferriage & Lindon, 1978). NMR spectra of the protein were obtained with samples containing 1.0 mM GVP, 55 mM NaCl, and 1 mM cacodylate, pH 7.0, in 99.75% D_2O. NMR samples of the protein–d$(A)_8$ complex contained 1.0 mM GVP, 0.6 mM d$(A)_8$, 55 mM NaCl, and 1 mM cacodylate, pH 7.2, in 99.75% D_2O. All spectra were recorded at 30 °C. In decoupling experiments, resonances were selectively irradiated by pulsed homonuclear decoupling to give decoupled spectra with a steady-state NOE. Nuclear Overhauser effects were measured by employing the pulse sequence [RD–Dec(t_1,ω_A)–FID(+)–RD–Dec(t_1,ω_{off})–FID(−)]$_n$. After a relaxation delay (RD) (1–2 s), a selective presaturation pulse of duration t_1 is applied by the ^{1}H decoupler at a chosen resonance A with resonance frequency ω_A. This is followed by the nonselective observation pulse, and the resultant FID is recorded. After a second relaxation delay, a presaturation pulse of the same duration t_1 is applied at an off-resonance position, ω_{off} (at the edge of the spectrum). Subtraction of the second FID from the first yields the NOE difference FID. The sequence is repeated appropriately for the desired signal-to-noise ratio. All measured NOE's were negative, but transformed NOE difference spectra were phased so as to give positive peaks. Contrary to the normal spectra, NOE difference spectra were not resolution enhanced.

The groups of Redfield (Johnston & Redfield, 1978; Stoetz et al., 1979) and Wüthrich (Wagner & Wüthrich, 1979; Dubs et al., 1979) have successfully employed this pulse sequence to measure selective NOE's in macromolecules. Essential is that the preirradiation pulse used is of sufficiently low power (40–50 dB below 0.1 W) to achieve selective saturation at site A and short enough to eliminate strong spin-diffusion effects outside the sphere of nearest neighbors to A. The optimal preirradiation time therefore depends on the molecular weight of the substance under investigation. In our case, a preirradiation time of 0.15 s was chosen. The preirradiation time was lengthened to 0.3 s for the observation of NOE's between the protein and the oligonucleotide.

Theoretical Section

The magnitudes of the Overhauser effects were calculated with the three-spin approximation of Wagner & Wüthrich (1979), which can be summarized by the following expression:

$$\frac{M_2}{M_1^0} = \frac{\sigma_{21}}{b-a}(e^{-at} - e^{-bt}) + \frac{\sigma_{21}\rho_3 - \alpha\sigma_{23}\sigma_{31}}{(a-b)ab}[be^{-at} - ae^{-bt} + (a-b)] + \frac{\sigma_{21}\rho_3 - \alpha\sigma_{23}\sigma_{31}}{(a-b)(b-c)(c-a)}[(b-c)e^{-at} + (c-a)e^{-bt} + (a-b)e^{-ct}] - \frac{\sigma_{21}}{(a-b)(b-c)(c-a)}[c(a-b)e^{-ct} + a(b-c)e^{-at} + b(c-a)e^{-bt}] \quad (1)$$

M_1^0 stands for the equilibrium magnetization minus the residual magnetization in the steady state of spin 1, which is saturated by the preirradiation pulse. $M_2 = M_{z2}(t) - M_z^{eq}$, where $M_{z2}(t)$ is the z component of the magnetization of the

observed spin 2 and M_z^{eq} is its equilibrium magnetization. Spin 3 is providing an additional relaxation mechanism for spin 2.

$$a = \tfrac{1}{2}\{(\rho_2 + \rho_3) - [(\rho_2 - \rho_3)^2 + 4\alpha\sigma_{23}^2]^{1/2}\} \quad (2a)$$

$$b = \tfrac{1}{2}\{(\rho_2 + \rho_3) + [(\rho_2 - \rho_3)^2 + 4\alpha\sigma_{23}^2]^{1/2}\} \quad (2b)$$

with

$$\rho_i = \frac{\hbar^2\gamma^4}{10}\sum_{j\neq i}\frac{1}{r_{ij}^6}\left[\tau_c + \frac{3\tau_c}{1+(\omega\tau_c)^2} + \frac{6\tau_c}{1+4(\omega\tau_c)^2}\right] \quad (3a)$$

$$\sigma_{ij} = \frac{\hbar^2\gamma^4}{10}\frac{1}{r_{ij}^6}\left[\frac{6\tau_c}{1+4(\omega\tau_c)^2} - \tau_c\right] \quad (3b)$$

where r_{ij} is the distance between protons i and j, ω is the Larmor precession frequency, and τ_c is the isotropic rotational correlation time. The constant c in eq 1 is given by $c = \frac{1}{2}(1/T_1 + 1/T_2)$ where T_1 and T_2 are the longitudinal and transverse relaxation times of proton 1. From the line widths, c is estimated to be 30 s^{-1}. Other symbols have their usual meaning. We have added the parameter α to account for the fact that spin 2 can be relaxed by more than one relaxing spin 3. In this derivation, it was assumed that α is time independent. For short times, this is a reasonable assumption. For longer times, this assumption is only justified if spin 2 experiences dipolar interaction equally to all spins 3. For example, when spin 2 is equally coupled to two spins 3, the factor α will be 2.

Calculation of the Overhauser effects for the aromatic ring protons requires some additional comments. Aromatic rings in proteins are not necessarily rigidly fixed to the molecular frame. For the gene-5 protein, we have good evidence that some of the tyrosyl and phenylalanyl rings are rapidly flipping around the C_β–C_γ bond (Garssen et al., 1980). In the calculations, two extreme situations have been considered. First, tyrosyl and phenylalanyl residues are assumed to rapidly reorientate about the C_β–C_γ bond. As a result, the 2 and 6 and the 3 and 5 ring protons, which are symmetrically related by a 180° flip around this axis, become equivalent and resonate at the same frequency. In that situation, the 2,6 protons (or the 3,5 protons) will be affected to the same extent by a preirradiation pulse, and these spins can be considered as a pseudo-one-spin system. Second, if the reorientation of the rings is slow relative to the chemical shift difference between protons 2 and 6 (or 3 and 5), the ring protons will, in general, be individually resolved. A preirradiation pulse at one of the ring protons 2 or 3 will not affect the other ring protons 6 or 5, if it is assumed that the reorientation is so slow that cross-saturation effects can be neglected. The most simple situation occurs when in the latter case proton 4 in the phenylalanyl ring is irradiated. Then an NOE can be observed on the 3 and 5 protons (spin 2 in eq 1), while the 2 and the 6 protons serve as the neighboring relaxing spins, respectively (spin 3 in eq 1). In most other situations, protons outside the aromatic rings will have to serve as the relaxing spin (spin 3). For instance, when a tyrosyl ring is rapidly rotating around the C_β–C_γ bond and the 3 and 5 protons are irradiated and the adjacent 2 and 6 protons are observed, then the β protons are considered to be the most obvious spins 3. In this particular case of rapid rotation, it can be shown easily that also the 2 and 6 protons as well as β protons can be approximated as pseudo-one-spin systems.

If on the other hand the ring is fixed with respect to the β protons while the 3 or the 5 ring proton is irradiated, then again the relaxing proton will be one of the β protons. However, due to the short distance between the β protons, they are strongly dipolar coupled, and to a good approximation the magnetizations of the two β protons will remain equal. In the calculation of the distance between a β proton and an aromatic ring proton, the plane of the ring is assumed to be parallel to the vector connecting the two β protons. This is the most probable conformation for an aromatic residue (Janin et al., 1978).

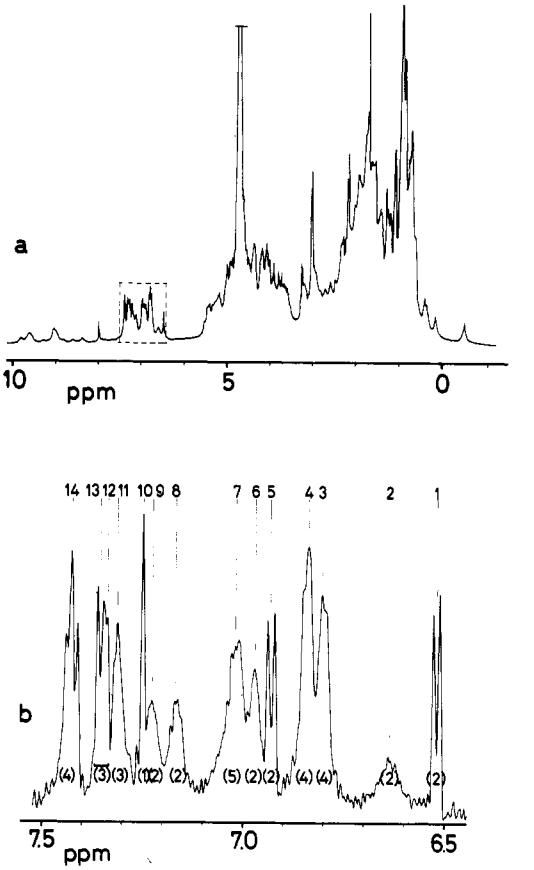

FIGURE 1: ^{1}H NMR spectrum (500 MHz) of GVP. In (a), the total protein spectrum is given. An expansion of the spectral region in the box is given in (b). Note that the C2 proton resonance at 8.03 ppm of the single histidine in the protein is not included in (b). Peaks are numbered 1–14. The number of protons resonating under each peak is given within parentheses.

Finally, one other situation has to be considered of which the following situation provides an example. When the 2 and/or 6 protons of a tyrosyl residue are preirradiated and the 3 and/or 5 protons are observed, then none of the protons within the tyrosyl residue is adequate to serve as the relaxing spin 3. We assume that there will always be a proton belonging to another residue near the observed proton. Therefore, in such cases, a hypothetical spin 3 at 3.5 Å from the observed proton was incorporated in the calculations.

Results and Discussion

Assignments. (a) Aromatic Part of the 500-MHz ^{1}H NMR Spectrum of GVP. In Figure 1a, the overview 500-MHz ^{1}H NMR spectrum of GVP is given. A resolution-enhanced expansion of the region 6.5–7.5 ppm, enclosed in the box in Figure 1a, is depicted in Figure 1b. As an aid in the discussion, the peaks have been numbered. The number of protons resonating at a certain spectral position is given within parentheses. These numbers were obtained by integrating the spectrum and taking signal 1 as a two-proton doublet. The total number of aromatic resonances expected on the basis of the aromatic amino acid content (5 Tyr, 3 Phe, and 1 His) is 37. One of these, the resonance of the C2 proton of His-64,

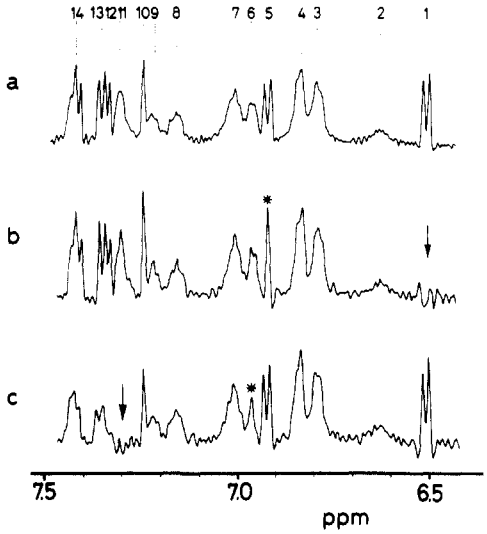

FIGURE 2: Selective decoupling experiments in the aromatic part of the 500-MHz ^{1}H NMR spectrum of GVP. Arrows indicate the spectral position at which irradiation was applied. Differences with respect to the undecoupled spectrum induced by the irradiation are marked with an asterisk. (a) Undecoupled spectrum; (b) irradiation of peak 1; (c) irradiation of peak 11.

resonates at 8.03 ppm (see Figure 1a) and falls outside the region displayed in Figure 1b.

Several of the resonances in the aromatic region have been assigned to distinct residues earlier (Garssen et al., 1978, 1980; Hilbers et al., 1978). Using the technique of photochemically induced dynamic nuclear polarization (photo-CIDNP), we assigned the doublet 1 at 6.52 ppm, as well as resonances in peaks 3 and 4, to the 3,5 ring protons of tyrosyl residues at the surface of the protein (Garssen et al., 1978). The assignments were further aided by the isolation and purification of a gene-5 protein in which the phenylalanines were deuterated. With the help of the spectrum of this protein, it could be shown that the peaks resonating below 7.3 ppm, i.e., peaks 11–14, arise from ring protons of phenylalanine (Hilbers et al., 1978; Garssen et al., 1980). Comparison of the spectrum at 500 MHz with the spectrum of the deuterated protein now allows us to assign resonance 9 and tentatively resonance 6 to phenylalanyl ring protons.

The interpretation of the aromatic spectrum can be extended by performing selective decoupling and NOE experiments, which are made possible by the improved resolution at 500 MHz.

(*b*) *Selective Decoupling in the Aromatic Spectrum of GVP.* All peaks in the aromatic spectrum were successively irradiated, and the resulting spectra were examined for differences with the undecoupled spectrum. For two reasons, we cannot expect that in all cases these decoupling experiments will reveal the coupling pattern of the lines. The first is that, in spite of the improved resolution, there are still a number of overlapping lines present in the spectrum. Second, the widths of some of the lines in the spectrum (e.g., peak 2 in Figure 1b) are much larger than the coupling constant of adjacent protons in phenylalanyl and tyrosyl rings ($J \simeq 7$–8 Hz). Decoupling of such lines is not expected to cause detectable changes in the spectrum.

In Figure 2, two examples of successful decoupling experiments are given. The irradiation frequency is indicated by an arrow, and the spectral changes caused by the irradiation are marked with an asterisk. Figure 2b shows the spectrum recorded during irradiation of doublet 1. As a result of the irradiation, peak 5, which is a doublet in the undecoupled spectrum (Figure 2a), has become a single line. Since peak 1 had been assigned already to the 3,5 ring protons of a surface tyrosine, it can be concluded from this experiment that peak 5 arises from the 2,6 protons of the same surface tyrosine. It should be noted in passing that the integrated intensity of peak 5 decreases when peak 1 is irradiated. This is a result of the (in this case negative) NOE that accompanies this kind of decoupling experiment. Figure 2c shows the spectrum recorded during irradiation of peak 11. The difference of this spectrum with the undecoupled spectrum (Figure 2a) is less pronounced. However, the narrowing of peak 6 as a result of the irradiation of peak 11 can only be explained if components of peak 11 and peak 6 are coupled. Since peak 11 was positively assigned to phenylalanyl ring protons, our tentative assignment of (at least part of) peak 6 to phenylalanyl protons is confirmed by this experiment (vide supra).

Table I: Decoupling Experiments in the Aromatic Part of the 500-MHz ^{1}H NMR Spectrum of GVP[a]

irradiation of peak number	effect on peak number
1	5
5	1
7	3
8	4
11	6
12	14
13	14
14	13

[a] Peak numbers correspond to those in Figure 1b. When one of the peaks not listed here was irradiated, no changes could be detected in the spectrum. The dashed lines indicate that a decoupling effect could be observed for either of the coupled resonances.

The results of the decoupling experiments are summarized in Table I. This table shows that the irradiation of eight of the fourteen peaks resulted in changes in the spectrum. The relatively narrow peaks, exhibiting clear splittings (peaks 1, 5, 13, and 14), lose (part of) their splitting pattern when a coupled resonance is irradiated. In these cases, effects of decoupling could be observed after irradiation of either of the coupled peaks. This is indicated in Table I by a dashed line. The results obtained for peaks 12, 13, and 14 indicate that these peaks contain resonances of one phenylalanyl residue, with the 2,6 protons resonating in peak 13, the 4 proton in peak 12, and the 3,5 protons in peak 14. This interpretation could be confirmed by a spin simulation of the phenylalanyl spectrum. Irradiation of peaks 7, 8, and 11 results in narrowing of peaks 3, 4, and 6, respectively. As is seen in Table I, no changes in peaks 7, 8, and 11 could be detected when peaks 3, 4, and 6 were irradiated. For peaks 7 and 8, this is understandable in view of the width of these peaks. The absence of decoupling effects on peak 11 will be discussed below.

(*c*) *Selective NOE in the Aromatic Spectrum of GVP.* If the experimental conditions are chosen properly, NOE's can be expected primarily on the protons in the aromatic rings that are adjacent to the preirradiated protons. In conjunction with the decoupling experiments discussed above, this permits a detailed interpretation of the spectrum. A first example of the effects, which can be expected, is presented in Figure 3.

In the NOE difference spectrum (see Materials and Methods) measured after preirradiation of resonance 1 (Figure 3a), an NOE is observed for resonance 5. This NOE is very specific; no other peaks appear in the difference spectrum. Since we already know that resonances 1 and 5 belong to the 3,5 and 2,6 protons of the same tyrosyl residue, this experiment demonstrates the magnitude of the NOE's that can be expected for adjacent protons in an aromatic ring. The reverse experiment, i.e., preirradiation of peak 5, results, as expected,

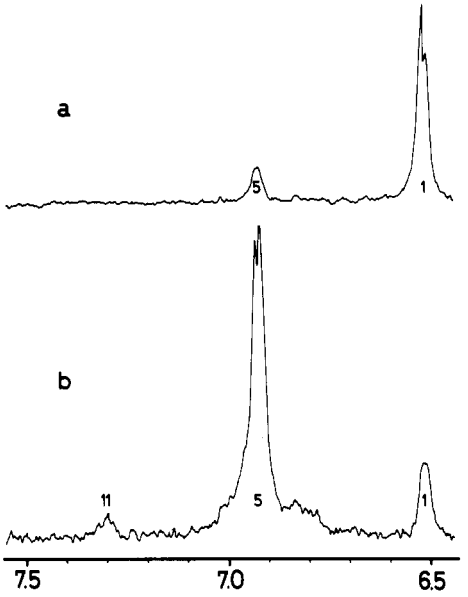

FIGURE 3: Aromatic part of the 500-MHz NOE difference spectrum of GVP. Peak numbers correspond to those in Figure 1b. The negative NOE's were phased so as to give positive peaks. (a) Peak 1 is preirradiated; an NOE is observed for peak 5. (b) Peak 5 is preirradiated; an NOE is observed for peak 1 and to a smaller extent for peak 11. The reason for the occurrence of the latter effect is explained in the text.

in an NOE for peak 1 (Figure 3b). In addition, a small effect is observed for peak 11. This additional NOE arises because of the overlap between peaks 5 and 6 (note that the spectrum in Figure 1b has been resolution enhanced). The preirradiation pulse applied to peak 5 also effects to some extent peak 6, which in turn gives rise to an NOE on peak 11. If there is no severe overlap of lines, as in this case, the additional NOE's are small and can be distinguished easily from the main NOE's. In cases of stronger overlap, this distinction can be made with the aid of the supplementary information provided by the reverse experiments.

This is demonstrated in Figure 4. Figure 4a shows that NOE's are observed for peaks 2, 7, and 8, when peak 3 is preirradiated. These effects are small compared with the intensity of peak 3 in the difference spectrum since peak 3 consists of resonances of four protons. The results of the reverse experiments were examined to determine whether one of the measured NOE's is due to the overlap of peak 3 with peak 4 (see Figure 1b). The NOE measured for peak 3 when peak 2 is preirradiated is shown in Figure 4b and confirms the coupling present between peaks 3 and 2. When peak 7 is preirradiated (Figure 4c), an NOE is observed for peak 3 and peak 4. This means that peak 7 indeed contains a resonance that is coupled with a component of peak 3. In addition, another resonance in peak 7 is probably coupled with a component of peak 4. The NOE difference spectrum recorded when peak 8 is preirradiated (Figure 4d) only shows an NOE for peak 4. It is therefore concluded that the effect measured for peak 8 in Figure 4a originates because of the partial overlap between peaks 3 and 4. Thus, the experiments shown in Figure 4 lead to the conclusion that the four resonances composing peak 3 are each coupled to either peak 2 or peak 7.

The results of the NOE experiments are summarized in Table II. The magnitude of the measured NOE is listed as

$$\frac{\text{area of observed peak in difference spectrum}}{\text{area of irradiated peak in difference spectrum}} \times \frac{}{\text{number of protons irradiated}}$$

In the ideal situation, that the peaks do not overlap, these values are equal to $-\sum_j M_j/M_1^0$ where the summation extends over all protons (all observed spins 2) that contribute to the observed NOE peak. The symbols used are the same as those in eq 1.

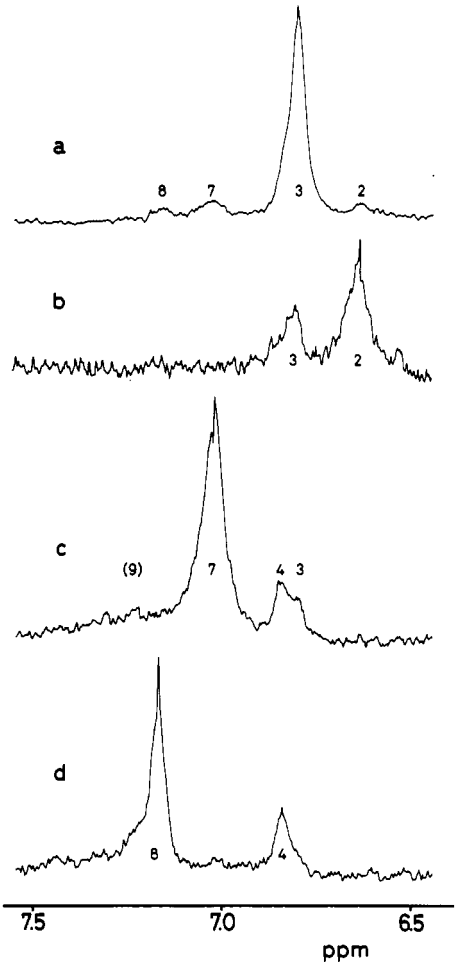

FIGURE 4: Aromatic part of the 500-MHz NOE difference spectrum of GVP. Peak numbers correspond to those in Figure 1b. The negative NOE's were phased so as to give positive peaks. (a) Peak 3 is preirradiated; NOE's are observed for peaks 2, 7, and 8. (b) Peak 2 is preirradiated; an NOE is observed for peak 3 only. (c) Peak 7 is preirradiated; NOE's are observed for peaks 3 and 4; a small effect might be present for peak 9 (see text). (d) Peak 8 is preirradiated; an NOE is observed for peak 4, but not for peak 3.

Table II: Selective NOE's in the Aromatic Part of the 500-MHz ^{1}H NMR Spectrum of GVP[a]

irradiated peak	obsd peak	NOE	obsd peak	NOE	obsd peak	NOE
1	5	0.37				
2	3	0.88				
3	7	(0.45)	8	(0.20)	2	(0.17)
4	7	(0.36)	8	(0.36)		
5	1	0.36	11	0.09		
6	11	(0.41)	1	(0.17)		
7	4	(0.59)	3	(0.55)	9	(0.09)
8	4	0.76				
9 + 10	14	0.55	7	0.23	4	0.17
11	6	(0.41)	14	(0.22)		
13	14	(0.62)	6/7	(0.08)		
14	12/13	(1.17)	9	(0.35)		

[a] Peak numbers correspond to those in Figure 1b. The listed values of the NOE's are equal to [(area of observed peak in difference spectrum)/(area of irradiated peak in difference spectrum)] × (number of protons irradiated). Underlined NOE's could be confirmed by a reverse experiment. The values within parentheses are not suited for comparison with calculated values because of peak overlap (see text).

Table III: NOE's Calculated by Using Equation 1[a]

label	residue	proton preirradiated	proton obsd	limit of flipping rate around C_β-C_γ bond[b]	NOE per proton $\tau_c = 8 \times 10^{-9}$ s	NOE per proton $\tau_c = 1.4 \times 10^{-8}$ s
A	Tyr	2 + 6	3 + 5	F	−0.204	−0.329
	Tyr	2 or 6	3 or 5	S		
B	Tyr/Phe	3 + 5	2 + 6	F	−0.183	−0.280
C	Phe	4	3 and/or 5	F/S	−0.189	−0.292
	Phe	3 or 5, 2 or 6	adjacent 4 or 3 or 5	S		
D	Phe	3 + 5	4	F	−0.363	−0.541
E	Phe	2 + 6	3 + 5	F	−0.186	−0.284
F	Tyr/Phe	3 or 5	2 or 6	S	−0.195	−0.307

[a] Assumptions in the calculations are described under Materials and Methods. The preirradiation time used in the calculations was 0.15 s. [b] F = fast; S = slow.

The observed NOE may deviate from its ideal value. In case of preirradiation of a peak consisting of several overlapping or partly overlapping resonances, the irradiation may saturate not all of the resonances to the same extent. As a result, too small a value for the NOE of protons coupled to the less saturated protons will be calculated and too large a value for the NOE of the remaining protons. This occurs when a preirradiation pulse is applied to peaks 3, 4, 7, or 14. Partial saturation of peaks adjacent to the irradiated one, due to peak overlap, will cause similar effects.

Therefore, the values of the NOE measured after irradiation of peaks that strongly overlap with other peaks or consist of more than three resonances are placed within parentheses in Table II. These values are not suited for a quantitative interpretation. The NOE's that could be confirmed by a reverse experiment are underlined. For the moment, we leave the exact values of the NOE's out of consideration, and for the reasons indicated above, we disregard the NOE's that could not be confirmed by a reverse experiment. If we then take all other NOE's to come from protons adjacent to the irradiated protons in the same aromatic ring, these results can be summarized as follows. In accordance with the conclusions derived from the decoupling measurements, peaks 1 and 5 and peaks 12, 13, and 14 are coupled. Furthermore, the results confirm the interrelations between peaks 7 and 3, peaks 8 and 4, and peaks 11 and 6 which were observed in the decoupling experiments only as a narrowing of a peak. In addition, the NOE experiments reveal several interactions that could not be detected in the decoupling experiments. These are the couplings between peaks 2 and 3, between peaks 4 and 7 already mentioned above, and a coupling between a component of peak 14 and peak 9. The NOE observed for peak 7 after irradiation of peaks 9 and 10 needs further comment. This effect cannot arise as a result of overlap of peaks 9 and 10 with peaks 8 or 11 since neither peak 8 nor peak 11 is coupled with peak 7. A reexamination of the NOE difference spectrum obtained after preirradiation of peak 7 (Figure 4c) discloses a small effect at the resonance position of peak 9. Therefore, we conclude that there is in fact a coupling between a component of peak 9 and a component of peak 7, the small value of the NOE being a result of overlap as outlined above.

(*d*) *Evaluation of the Magnitudes of the Overhauser Effects.* The values of the observed Overhauser effects contain information on the distance between the irradiated and the observed protons and in addition on the dynamics of the protein. As has been shown in the previous section, the Overhauser experiments were conducted in such a way that NOE's were only observed for protons adjacent to the irradiated proton(s). In order to see whether the observed effects are in accordance with theoretical expectations and to what extent dynamical effects are important, we have calculated the NOE's along the lines indicated in the theoretical section. Under our solution conditions, the gene-5 protein is expected to be present predominantly as a dimer. Sykes et al. (1978) have given an empirical relation between protein molecular weight and experimentally determined rotational correlation times from which we estimate a τ_c of about 10^{-8} s for the gene-5 protein dimer. In order to obtain an impression of the sensitivity of the NOE's for variation of τ_c around this value, NOE's were calculated for $\tau_c = 8 \times 10^{-9}$ s and $\tau_c = 1.4 \times 10^{-8}$ s and listed in Table III. All possible combinations of preirradiated and adjacent observed aromatic protons were examined while also the absence or presence of rapid rotation was taken into account (see Materials and Methods for a further description). From the calculated NOE's collected in Table III, it is clear that under the conditions chosen the effects are mainly determined by the distance between the irradiated proton(s) and the observed proton and by the rotational correlation time rather than by the influence of the relaxing spin 3. For case D, where the phenylalanyl 3,5 protons are preirradiated and the 4 proton is observed, a notably larger NOE is calculated. This is obviously caused by the fact that the observed proton is coupled to two preirradiated protons.

The dependence of the calculated NOE on the preirradiation time and on the rotational correlation time is shown in Figure 5a,b. The curves are marked corresponding to the labels in Table III. For the reasons mentioned above, curve D differs from the curves for all other cases over the whole range of τ_c's and preirradiation times. The difference between curves A and B is caused by the different distances to the relaxing spin 3. Figure 5a demonstrates that for short preirradiation times the NOE is mainly determined by the rate of magnetization transfer from the preirradiated proton to the observed proton, except for an initial lag phase due to the time it takes to saturate spin 1. Figure 5b shows that for a preirradiation time of 0.15 s the magnitude of the calculated NOE varies from ~0.1 to ~0.9 with τ_c increasing from 10^{-9} to 10^{-7} s. The calculated values in Table III can now be compared with the experimental results listed in Table II. As pointed out above, only the values without parentheses can be used to this end. Moreover, it should be realized that in Table III the Overhauser effects are given per proton whereas in Table II the total observed NOE at a given resonance position is listed. If we transfer the results of Table II to a one-proton Overhauser effect, we find for resonances 1 and 5, which are from the 3,5 and 2,6 protons of the same tyrosine, respectively, an NOE of 0.185. This is close to the value expected for a rotational correlation time $\tau_c = 8 \times 10^{-9}$ s (see Table III, A and B). On the other hand, irradiation of resonance 2 which comes from a tyrosine that is not at the surface of the protein leads to an

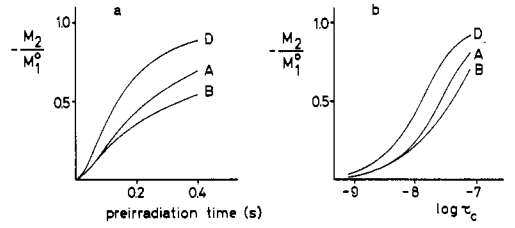

FIGURE 5: NOE's calculated with eq 1 for the situations labeled A, B, and D in Table III. (a) As a function of the preirradiation time with $\tau_c = 1.4 \times 10^{-8}$ s, $c = 30$ s^{-1}; (b) as a function of the rotational correlation time with $c = 30$ s^{-1} and a preirradiation time of 0.15 s.

NOE of 0.44 on resonance 3, which corresponds with $\tau_c = 2.5 \times 10^{-8}$ s (compare Figure 5b). Similar conclusions follow for the Overhauser effect observed for peak 4 after irradiation of peak 8. Again, we find a τ_c of about 2.5×10^{-8} s. As the overall rotational correlation time of the protein is expected to be equal to or larger than the largest rotational correlation time measured, this value for τ_c may indicate that the protein is aggregated somewhat beyond the dimeric state. It is interesting to note that tyrosine I, which is at the surface of the protein, has a correlation time which is shorter than those of the tyrosines expected to be in the interior of the protein. In relation to this, it should be realized that the kinetics of the 180° flips around the C_β–C_γ bond of an aromatic residue have no influence on the effective τ_c measured via Overhauser effects between adjacent 2,6 and 3,5 protons because the interproton dipolar interaction vector is parallel to the C_β–C_γ bond.

(*e*) *Complete Interpretation of the Aromatic Spectrum of GVP.* Combination of the data obtained in the various experiments described leads to a complete interpretation of the aromatic part of the spectrum, which is presented in Figure 6, above the spectrum in Figure 6a. The residues are numbered arbitrarily. The number of protons of a residue at a given resonance position is denoted in italics. We shall go through the spectrum residue by residue. The assignment of peaks 1 and 5 to tyrosine I needs no further discussion. The NOE experiments showed that peak 2 was coupled exclusively to peak 3 (Figure 4b, Table II). Therefore, we assign peak 2 and part of peak 3 to tyrosine II. Peak 8 and part of peak 4 are named tyrosine III, as the coupling between them was observed both in the decoupling and in the NOE experiments. In the decoupling experiments, a coupling between peaks 7 and 4 was observed while the NOE experiments showed that peak 7 is coupled both to peak 4 and to peak 3. In temperature-dependent experiments, we observed that a two-proton intensity in peak 3 shifts to low field upon raising the temperature and that two protons situated in the low-field flank of peak 7 do the same (data not shown). The resonances in peak 4 are temperature independent. We therefore attribute the temperature-dependent components of peaks 7 and 3 to a tyrosine numbered IV and the coupled parts of peak 7 and peak 4 to a tyrosine numbered V. All five tyrosines in the protein have now been assigned, and they account for the whole intensity of peaks 1–8 except for the intensity of peak 6 and a one-proton intensity in peak 7, in accordance with our earlier measurements on GVP with deuterated phenylalanines (Garssen et al., 1980). Peak 10 is a one-proton singlet and can be assigned to the C4 proton of His-64.

The only phenylalanyl resonances that are narrow enough to show *J* couplings are peaks 14, 13, and 12. Both the decoupling experiments and the NOE experiments indicate that the 3,5 protons of this phenylalanine I resonate in peak 14, the 2,6 protons in peak 13, and the 4 proton in peak 12, which was also confirmed by a spin simulation. The 3,5 protons of

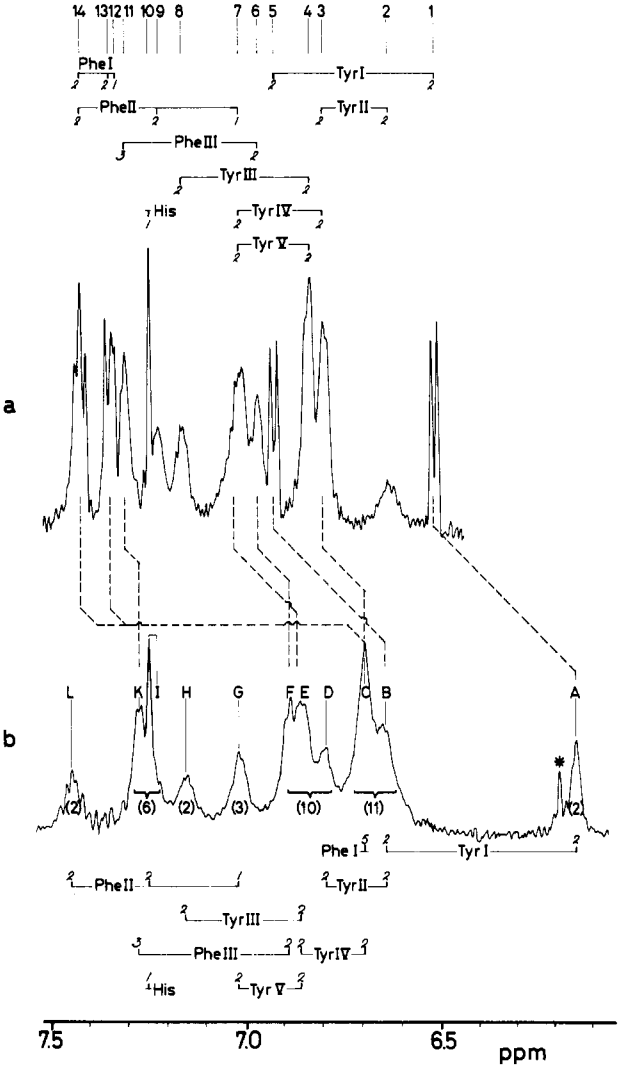

FIGURE 6: Comparison of the aromatic part of the 500-MHz ^{1}H NMR spectra of the free protein (a) and the protein–d(A)$_8$ complex (b). Prominent shifts are indicated with dashed lines. The interpretation of the spectra is given above (a) and underneath (b). Residue numbers are arbitrary, but a particular residue has the same number in (a) and (b). The number of protons of a certain residue resonating at the indicated position is given in italics. The peaks labeled A–L in the spectrum of the protein–d(A)$_8$ complex are protein resonances. The triplet marked with an asterisk belongs to an H_1' sugar proton of the d(A)$_8$. The number of protons resonating at a certain spectral position is denoted within parentheses.

phenylalanine I cannot account for the whole intensity of peak 14. It is therefore not surprising that the NOE experiments show that peak 14 is also coupled to peak 9. Peak 9 is coupled to peak 7 in which still a one-proton intensity was missing. We will therefore assign peak 9, two protons in peak 14, and one proton in peak 7 to a phenylalanine numbered II.

The only remaining intensity is situated in peaks 11 and 6, which were shown to be mutually coupled in the decoupling and in the NOE experiments. These peaks are therefore assigned to phenylalanine III. This phenylalanine deserves some extra attention. Peak 6 is too narrow to contain a two-proton doublet, and peak 11 would be expected to show some splitting. We can only reconcile the shape of both lines with the results of the described experiments when we suppose that ring protons 2 and 3 (or 6 and 5) resonate in peak 6 and ring protons 4, 5, and 6 (or 2, 3, and 4) in peak 11. A spin simulation confirms this interpretation. In that case, only one proton in peak 11 is coupled with a proton in peak 6, which explains why no decoupling effects could be detected in peak

11 when peak 6 was irradiated. This interpretation implies that phenylalanine III reorientates slowly about the C_β–C_γ bond and is probably situated in the interior of the protein.

Complex of GVP with d(A)$_8$. The aromatic part of the GVP spectrum changes completely when an excess of the oligonucleotide d(A)$_8$ is added. This is demonstrated in Figure 6, where the aromatic spectrum of the protein (Figure 6a) is compared with the spectrum of the protein–d(A)$_8$ complex (Figure 6b). The increased line widths in the latter spectrum indicate that the complex has a larger molecular weight than that of the free protein. The peaks labeled A–L in Figure 6b are protein resonances. The numbers within parentheses indicate the number of protons resonating at a certain spectral position. These numbers were obtained by integrating the spectrum, taking peak A as a two-proton peak. The triplet at 6.21 ppm marked with an asterisk is an H_1' sugar proton of the oligonucleotide. The adenyl ring protons resonate below 7.5 ppm.

From earlier experiments (Hilbers et al., 1978; Garssen et al., 1980), it could be concluded that the tyrosyl peak 1 and phenylalanyl resonances around 7.3 ppm in the spectrum of the free protein shift to high field when the protein binds to nucleotide. We can therefore conclude in advance that peak A in the spectrum of the complex (Figure 6b) corresponds to peak 1 in the free protein spectrum (Figure 6a). The spectrum of the complex could be further interpreted by proceeding in two ways. The first was to titrate the protein with d(A)$_8$ and other oligonucleotides and to follow the shifting resonances (details will be described elsewhere). During the titration, the free protein is in fast exchange with the protein in the complex. These titration experiments, which were performed at 360 MHz, lead to the conclusion that the resonances undergoing the largest shifts are those arising from the residues designated in Figure 6a as Phe I, Tyr I, and Tyr IV (see dashed lines in Figure 6). In addition, it followed that the histidyl proton resonances remain at their positions upon complex formation.

In the second approach, NOE experiments were performed as for the free protein. In this way, the results mentioned above could be confirmed and the remaining part of the spectrum interpreted. In order to obtain satisfactory signal-to-noise ratios in these NOE experiments, the same experimental conditions were used as for the free protein. The preirradiation time of 0.15 s is fairly long to be used for the complex, because the enhanced spin diffusion can lead to less specific saturation transfer. Loss of specificity is also caused by the strong overlap of lines. Because of this, a quantitative discussion of the magnitudes of the measured effects is in most cases not possible. A qualitative discussion of the results nevertheless permits a detailed interpretation of the spectrum of the protein–d(A)$_8$ complex. Measured NOE's are listed in Table IV as strong (s) or weak (w) effects. As in the NOE experiments performed on the free protein, we will only take in consideration the NOE's that could be confirmed by a reverse experiment (underlined in Table IV). We shall first discuss the resonances that do not shift upon complex formation.

Preirradiation of the resolved peak L gives rise to a very specific NOE at peak I, and the magnitude is indicated in Table IV. Note that the C4 proton of the single histidine in the protein, which, as mentioned above, does not shift upon complex formation, also contributes to peak I. Since the resonance positions of peaks L and I correspond to peaks 14 and 9 in the free protein, we can (tentatively) conclude that peaks L and I belong to the phenylalanyl residue, designated Phe II in the preceding section. This conclusion is strengthened by the observation that upon irradiation of peak I NOE's are

Table IV: Selective NOE's in the Aromatic Part of the 500-MHz ^{1}H NMR Spectrum of the GVP–d(A)$_8$ Complex[a]

preirradiated peak	obsd peaks
A	B s (0.47)
B	A s, D s
D	B/C s, E s, K w, H w, G w
E	B/C s, K s, H w, G w
F	K s, B/C w
G	E s, I w
H	E s, I w
I	L s, F s, G w
K	F s, L w, G w
L	I s (0.98)

[a] Peak labels correspond to those in Figure 6b. Underlined NOE's could be confirmed by a reverse experiment. The magnitudes of the NOE's are indicated as strong (s) or weak (w). The magnitudes of the NOE's observed after preirradiation of peaks A and L could be evaluated quantitatively and are given in addition.

observed for peak L and peak G (see Table IV). The latter resonance has the same position as peak 7, part of which in the spectrum of the free protein was assigned to this same phenylalanine II. Peaks H and E turn out to be strongly coupled. Their positions correspond to those of peaks 8 and 4 in the free protein; these peaks are also strongly coupled (see Table II) and were assigned to a tyrosine named Tyr III. Hence, we conclude that the resonances of this residue do not shift upon complex formation. On the basis of identical arguments, the same conclusions were drawn for Tyr II (resonance D and part of resonance B) and for tyrosine V (part of resonance G and of resonance E); details can be found in Figure 6 and Table IV. The resonances of phenylalanine III undergo only small shifts upon complex formation, peaks K and F corresponding to peaks 11 and 6. The resonances of the remaining residues, namely, Tyr I, Tyr IV, and Phe I, shift significantly upon complex formation. This has been discussed already for Tyr I, which gives rise to peak A and part of peak B in the spectrum of the complex. For the other two residues, this is concluded from the titration experiments mentioned above. The resonances of Phe I can be seen to shift from the position of peaks 14, 13, and 12 to the position of peak C while the ring protons of Tyr IV, contributing originally to peaks 7 and 3, most likely resonate in peaks E and C. Unfortunately, peak C was not preirradiated so that the NOE observed for peak C after preirradiation of peak E has not been confirmed by a reverse experiment. The interpretation of the aromatic spectrum of the protein–d(A)$_8$ complex is given schematically under the spectrum in Figure 6b. The residue numbers correspond to those used in the interpretation of the free protein spectrum (Figure 6a). The shifts that appear in the spectrum upon binding of d(A)$_8$ are indicated in Figure 6 with dashed lines. This interpretation implies that Phe I, Tyr I, and probably Tyr IV are involved in the DNA binding. The small shifts undergone by the resonances of Phe III can be attributed to an indirect effect of a protein conformational change.

The fact that the interactions of the nonshifting resonances observed in the NOE experiments performed with the complex correspond with those in the spectrum of the free protein gives us confidence in the general correctness of this interpretation. Yet, we present this interpretation with some reservation because of the severe peak overlap in the spectrum of the complex. Also, it was assumed that the kinetics of the 180° flips of the aromatic rings do not change significantly upon complex formation. If such a change occurs, details of the interpretation may need to be readjusted.

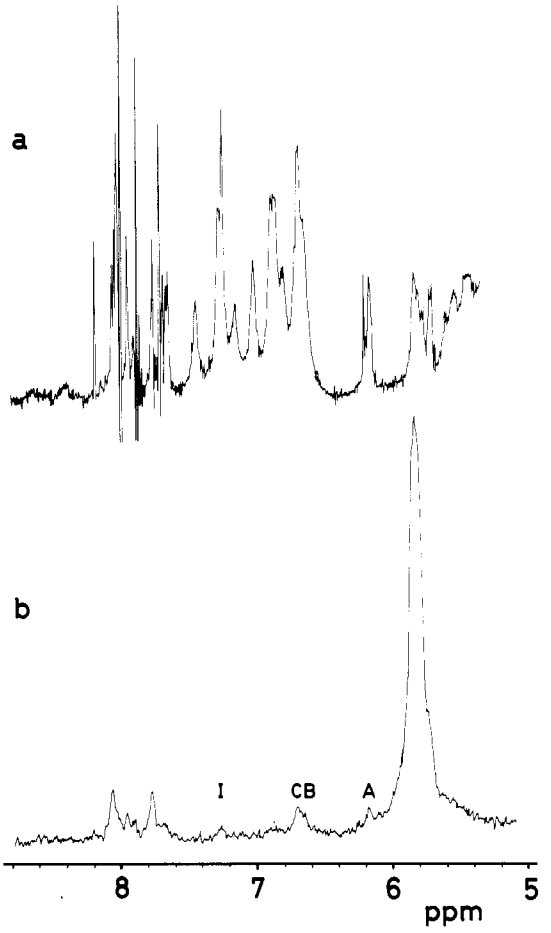

FIGURE 7: (a) ^{1}H NMR spectrum (500 MHz) of the GVP–d(A)$_8$ complex recorded between 5.4 and 8.8 ppm downfield from DSS. (b) NOE difference spectrum of the GVP–d(A)$_8$ complex. A preirradiation pulse of 0.3 s was applied to a peak at 5.84 ppm consisting of resonances of the H_1' sugar protons of d(A)$_8$. NOE's are observed for peaks I, C/B, and A (lettering as in Figure 6b) and resonances between 7.6 and 8.2 ppm belonging to base protons of the d(A)$_8$.

The NOE experiments were extended by preirradiating resonances of the oligonucleotide. When the H_1' sugar protons at 5.84 ppm were preirradiated, small but specific and reproducible NOE's could be observed for some protein resonances. Figure 7b shows the NOE difference spectrum obtained in this experiment. For comparison, a spectrum of the protein–d(A)$_8$ complex is given in Figure 7a. The NOE's observed below 7.6 ppm arise from adenyl protons of the oligonucleotide. Considerable Overhauser effects were also observed for sugar protons H_2', H_4', and H_5' resonating at higher field (not shown). The protein peaks exhibiting NOE's are peaks I, B/C, and A (note that the latter is not coming from the H_1' sugar proton starred in Figure 5b which resonates at slightly lower field). Interestingly, peaks A and B/C contain just those protein resonances that have undergone the largest shifts upon complex formation (vide supra). For the same protein resonances, somewhat smaller NOE's were observed after preirradiation of the adenyl resonance at 8.06 ppm for which an NOE was observed in Figure 7b. Preirradiation of the adenyl resonance at 7.78 ppm, which gives rise to the other predominant adenyl NOE in Figure 7b, results in an NOE on peaks I and B/C but not on A. After preirradiation of both adenyl peaks, NOE's were found for the sugar H_1' protons and for H_2', H_3', H_4', and H_5' sugar resonances.

While the NOE for peak A can be assigned to the 3,5 protons of Tyr I, we cannot unequivocally determine which residue gives rise to the NOE's observed for peaks I and B/C. It is, however, most likely that the resonances of phenylalanine I and/or those of tyrosine IV which have undergone large shifts upon complex formation (Figure 6) are responsible for the NOE for peak B/C.

In order to observe these NOE's, the preirradiation time had to be lengthened to 0.3 s. The magnitude of the NOE is a factor of 20–50 smaller than would be expected for adjacent protons in an aromatic ring under these experimental conditions. Because the effects are small and the preirradiation time is fairly long, there is a possibility that the observed NOE's for the protein resonances are secondary effects. This is indeed indicated by the observation that preirradiation of the protein peaks A, B/C, and I, using the same lengthened preirradiation pulse, does not result in NOE's for the sugar H_1' and adenyl protons. Instead, small effects were observed at the resonance positions of the H_3', H_4', and H_5' protons. At the same resonance positions, considerable NOE's were observed after preirradiation of the sugar H_1' and adenyl ring protons. Hence, we conclude that the NOE's for protein resonances observed after preirradiation of the sugar H_1' and adenyl ring protons are induced via the H_3', H_4', and/or H_5' sugar protons. Preirradiation at these resonance positions cannot yield an unambiguous verification for this conclusion, because the C_α protons of the protein also resonate in this spectral region. Irrespective of which of the protons of the d(A)$_8$ is nearest to the protein, we can conclude from these NOE experiments that the oligonucleotide is located near the aromatic protons of Tyr I and (most likely) of Phe I and/or of Tyr IV. According to the X-ray diffraction data obtained for the gene-5 protein (McPherson et al., 1979, 1980b), four tyrosyl residues (26, 34, 41, and 56) can be located in the DNA binding groove. Our data indicate that two of these tyrosines (designated Tyr I and Tyr IV in the present paper) are actually interacting with DNA. In the X-ray structure, Tyr-41, Tyr-34, and Phe-13 seem to stack upon each other, Tyr-34 being interposed between Tyr-41 and Phe-13. In such a configuration, the resonances of Tyr-34 and Tyr-41 would be expected to shift upfield due to the ring current effects of their neighbors and therefore are candidates for Tyr I of which the resonances have shifted upfield. Since in nitration experiments Tyr-34 was not nitrated in contrast to Tyr-41 (Anderson et al., 1975) and since Tyr I has been shown to be available for dyes that are able to induce photochemically induced nuclear polarization (Garssen et al., 1978), Tyr I may correspond with Tyr-41. Tyr IV will then correspond with Tyr-26, Tyr-34, or Tyr-56. With respect to the phenylalanines, the X-ray data suggest that both Phe-13 and Phe-68 are able to interact with the DNA. It is therefore tempting to conclude that either Phe-13 or Phe-68 corresponds with Phe I. Chemical modification experiments or additional double-resonance experiments are needed to establish these points.

Conclusions

The 500-MHz ^{1}H NMR spectra of GVP display an improved resolution with respect to those obtained at 360 MHz. This allowed us to perform selective NOE and decoupling experiments in the aromatic spectra of GVP. With the aid of these techniques, a complete assignment of the resonances of the aromatic ^{1}H spectrum to the different types of aromatic residues present in the protein could be made for GVP free in solution as well as for the protein–d(A)$_8$ complex. On the basis of these assignments, it could be concluded that at least one aromatic residue (Phe III) reorientates slowly about the C_β–C_γ bond. The next stage of the interpretation of the spectrum will be the assignment of the resonances to particular residues in the amino acid sequence. Calculation of the NOE's in a three-spin approximation (Wagner & Wüthrich, 1979)

shows that under our experimental conditions the NOE's between adjacent protons in the aromatic rings are not very sensitive to the exact distance of the relaxing proton 3 so that the effects are determined mainly by the crossrelaxation rate between the preirradiated and the observed proton. However, the effects are strongly dependent on the rotational correlation time τ_c, and, therefore, differences in NOE's observed for resolved resonances can be attributed to different mobilities of the residues. On this basis, it turns out that Tyr I is more mobile than Tyr II. This is in correspondence with our earlier observations that Tyr I is situated at the surface of the protein while Tyr II was expected to be in the interior of the protein (Garssen et al., 1978). Two of the five tyrosines in GVP, namely, Tyr I and Tyr IV, are involved in complex formation with $d(A)_8$. A phenylalanyl residue (Phe I) is also involved in complex formation. Its narrow resonances suggest that it has a considerable degree of motional freedom so that we expect it to be also situated at the protein surface. The shifts observed after complex formation strongly indicate the stacking of the aromatic rings of Phe I, Tyr I, and Tyr IV on the adenyl rings. In part, such conclusions have been drawn in earlier work (Hilbers et al., 1978; Garssen et al., 1980; Coleman & Armitage, 1978). The observation of such shifts does not guarantee however that these aromatic residues are really situated in the DNA binding groove. Direct evidence for the proximity of protons of the oligonucleotide and aromatic ring protons of the protein could be obtained in NOE experiments. In these NOE experiments, magnetization transfer was observed from sugar H_3', H_4', and/or H_5' protons of the oligonucleotide to aromatic protons of Tyr I and (most likely) Phe I and/or Tyr IV.

Acknowledgments

We thank Professor Dr. J. G. G. Schoenmakers and Dr. R. H. N. Konings for stimulating discussions. C. Prinse is acknowledged for her skillful technical assistance in the preparation of GVP.

References

Alberts, B., Frey, L., & Delius, H. (1972) *J. Mol. Biol. 68*, 139–152.

Anderson, R. A., Nakashima, Y., & Coleman, J. E. (1975) *Biochemistry 14*, 907–917.

Arentzen, R., Van Boeckel, C. A. A., van der Marel, G., & van Boom, J. H. (1979) *Synthesis*, 137–139.

Böttcher, C. J. F., Van Gent, C. M., & Pries, C. (1971) *Anal. Chim. Acta 24*, 203–204.

Cavalieri, S. J., Neet, K. E., & Goldthwait, D. A. (1976) *J. Mol. Biol. 102*, 697–711.

Coleman, J. E., & Armitage, I. M. (1977) in *NMR in Biology* (Dwek, R. A., Campbell, I. D., Richards, R. E., & Williams, R. J. P., Eds.) pp 171–200, Academic Press, New York.

Coleman, J. E., & Armitage, I. M. (1978) *Biochemistry 17*, 5038–5045.

Coleman, J. E., Anderson, R. A., Ratcliffe, R. G., & Armitage, I. M. (1976) *Biochemistry 15*, 5419–5430.

Cuyper, T., Van der Ouderaa, F. J., & De Jong, W. W. (1974) *Biochem. Biophys. Res. Commun. 59*, 557–564.

Day, L. A. (1973) *Biochemistry 12*, 5329–5339.

Dubs, A., Wagner, G., & Wüthrich, K. (1979) *Biochim. Biophys. Acta 577*, 177–194.

Ernst, R. R. (1966) *Adv. Magn. Reson. 2*, 1–135.

Ferrige, A. G., & Lindon, J. C. (1978) *J. Magn. Reson. 31*, 337–340.

Garssen, G. J., Hilbers, C. W., Schoenmakers, J. G. G., & van Boom, J. H. (1977) *Eur. J. Biochem. 81*, 453–463.

Garssen, G. J., Kaptein, R., Schoenmakers, J. G. G., & Hilbers, C. W. (1978) *Proc. Natl. Acad. Sci. U.S.A. 75*, 5281–5285.

Garssen, G. J., Tesser, G. I., Schoenmakers, J. G. G., & Hilbers, C. W. (1980) *Biochim. Biophys. Acta 607*, 361–371.

Hilbers, C. W., Garssen, G. J., Kaptein, R., Schoenmakers, J. G. G., & van Boom, J. H. (1978) in *Nuclear Magnetic Resonance Spectroscopy in Molecular Biology* (Pullman, B., Ed.) pp 351–364, Reidel, Dordrecht, The Netherlands.

Janin, J., Wodak, S., Levitt, M., & Maigret, B. (1978) *J. Mol. Biol. 125*, 357–386.

Johnston, P. D., & Redfield, A. G. (1978) *Nucleic Acids Res. 5*, 3913–3927.

McPherson, A., Jurnak, F. A., Wang, A. H. J., Molineux, I., & Rich, A. (1979) *J. Mol. Biol. 134*, 379–400.

McPherson, A., Wang, A. H. J., Jurnak, F. A., Molineux, I., Kolpak, F., & Rich, A. (1980a) *J. Biol. Chem. 255*, 3174–3177.

McPherson, A., Jurnak, F. A., Wang, A., Kolpak, F., Rich, A., Molineux, I., & Fitzgerald, P. (1980b) *Biophys. J. 32*, 155–173.

Nakashima, Y., Dunker, A. K., Marvin, D. A., & Konigsberg, W. (1974a) *FEBS Lett. 40*, 290–292.

Nakashima, Y., Dunker, A. K., Marvin, D. A., & Konigsberg, W. (1974b) *FEBS Lett. 43*, 125.

Oey, J. L., & Knippers, R. (1972) *J. Mol. Biol. 68*, 125–138.

Pratt, D., Laws, P., & Griffith, J. (1974) *J. Mol. Biol. 82*, 425–439.

Pretorius, H. T., Klein, M., & Day, L. A. (1975) *J. Biol. Chem. 250*, 9262–9269.

Ray, D. S. (1977) *Compr. Virol. 7*, 105–178.

Stoetz, J. D., Malinowski, D. P., & Redfield, A. G. (1979) *Biochemistry 18*, 4669–4675.

Sykes, B. D., Hull, W. E., & Snyder, G. H. (1978) *Biophys. J. 21*, 137–146.

Wagner, G., & Wüthrich, K. (1979) *J. Magn. Reson. 33*, 675–680.